Mechanisms of Interactive Crazing in PC/SAN Microlayer Composites

K. SUNG, D. HADERSKI, A. HILTNER,* and E. BAER

Department of Macromolecular Science and Center for Applied Polymer Research, Case Western Reserve University, Cleveland, Ohio 44106

SYNOPSIS

Mechanisms are proposed for the two types of interactive crazing that have been observed in PC/SAN microlayer composites when the PC layer thickness is on the micron-size scale. It is demonstrated that when the PC layer is thin enough the deformation zone that forms at a craze tip can interact with the next-neighboring SAN layer. By measuring the dimensions of the craze tip in scanning electron micrographs, it was found that the craze-tip opening does not depend on the SAN layer thickness, i.e., the length of the SAN craze. Consequently, the size and shape of the resulting plastic zone in the PC layer are also independent of layer thickness. The zone that forms in the PC layer consists of a colinear plastic zone together with a pair of micro-shearbands that grow at an angle of about 45°. When the PC layer is less than 6 μm, the elastic stress concentration from the colinear plastic zone increases the probability of crazing in the neighboring SAN layer with the formation of craze doublets that consist of two aligned crazes in neighboring SAN layers. By taking into consideration the Weibull distribution of crazing, a craze doublet fraction comparable to the 30% observed experimentally was predicted with a stress intensification factor in the range of 1.03–1.05. When the PC layer thickness is less than 1.3 μm, the length of the colinear plastic zone is comparable to the PC layer thickness. Formation of a craze at the point of impingement of the plastic zone on the neighboring SAN layer leads to craze arrays with many aligned crazes in neighboring SAN layers. At higher strains, the micro-shearbands grow through the PC layers and extend into several adjacent SAN and PC layers. This produces a change in deformation mechanism in the SAN layers at the yield instability, from craze opening to shear yielding. © 1994 John Wiley & Sons, Inc.

INTRODUCTION

Previous studies have shown that interactive crazing phenomena in the SAN layers of polycarbonate/styrene–acrylonitrile copolymer (PC/SAN) microlayer composites depend only upon the thickness of the PC layer.[1] When the PC layer is on the size scale of tens of microns, crazing occurs randomly with no registry of crazes from one SAN layer to the next. Interactive crazing in the form of craze doublets and craze arrays is observed when the PC layer thickness is decreased to several microns or tenths of microns.

Interactive shear processes are also observed in the microlayer composites.[2,3] Initiation of micro-shearbands at the craze tips eventually terminates crazing. The micro-shearbands subsequently grow through several alternating PC and SAN layers when the layers are thin enough. Interactive shear deformation produces a transition in the deformation mechanism of the SAN layers that is responsible for increased ductility and toughness of composites with thinner layers.

It is supposed that when the PC layer is thin enough, the redistributed stress field created by the impingement of the craze tip on the SAN/PC interface extends through the PC layer and influences crazing and micro-shearbanding in the next-neighboring SAN layer. The craze-tip deformation zone in the PC layer was characterized in a microlayer composite with relatively thick layers where the deformation zone was small compared to the thickness of the PC layer and the zone did not extend to the

* To whom correspondence should be addressed.

Journal of Applied Polymer Science, Vol. 52, 147–162 (1994)
 CCC 0021-8995/94/020147-16

next SAN layer.[4] The deformation zone at the blunted craze tip was amenable to the same analysis as the macroscopic zone that forms in PC at the root of a semicircular notch. Using the macroscopic concepts, the craze-tip deformation zone can be described by two plane strain shear yielding modes: core yielding and hinge shear.

The concepts of the craze-tip deformation zone are extended in the present study to describe the mechanisms of interacting crazing and microshearbanding in PC/SAN microlayer composites with thin layers. The study focuses on microlayer composites with layer thicknesses less than 10 μm. Specifically, two ranges in the thickness of the PC layers are of interest: 1.3–6 μm, where craze doublets are observed, and less than 1.3 μm, where virtually all the crazes are in craze arrays.

MATERIALS AND METHODS

Microlayer composites in the form of coextruded sheets were provided by The Dow Chemical Co. The microlayer composites were composed of alternating layers of two immiscible polymers, polycarbonate (PC) and a styrene–acrylonitrile copolymer (SAN) with 25% acrylonitrile by weight. The outermost layer was PC in all cases. The individual layer thicknesses of PC and SAN were changed by varying the total number of layers, from 49 to 1857, and the volume ratio of the two components. The thickness of the sheets was in the range of 1.1–1.4 mm. The composition of the composites was described by PC and SAN layer thicknesses. The average layer thicknesses were measured from optical micrographs and scanning electron micrographs.

Microspecimens with a thickness of 0.8 mm were sectioned from the edge of the coextruded sheet with a low-speed diamond saw (Isomet, Buehler Ltd.). The surfaces were polished on a metallurgical polishing wheel initially with 1200 and 2400 grit wet sandpapers and subsequently with 1.0 and 0.3 μm alumina aqueous suspensions. A thinner gauge section was prepared by polishing to a thickness between 0.4 and 0.6 mm.

The polished specimen was clamped in a microtensile tester (Minimat, Polymer Laboratories) for uniaxial tensile testing. The miniature materials tester was mounted on the stage of an optical microscope (Olympus BH2). The specimen was periodically photographed as it was extended at a rate of 0.01 mm/min.

For scanning electron microscopy (SEM), the specimen was first deformed in the Minimat to a selected strain, then reloaded to the same strain on a modified SEM tensile stage. The restretched specimen was coated with a 30 Å layer of gold and observed under load in the low-voltage scanning electron microscope (JEOL JSM-840A).

RESULTS AND DISCUSSION

Craze-tip Opening

Typical examples of the craze-tip region of the three types of crazes observed in PC/SAN microlayer composites, specifically, a single craze, a craze from a craze doublet, and a craze from a craze array, are compared in Figure 1. The tip of a single craze in 49-layer PC/SAN (29/16 μm) strained to about 4.5% is shown in Figure 1(a). Good adhesion between SAN and PC prevented delamination where the SAN craze impinged on the interface. The craze did not grow through the interface into the PC layer; instead, the craze tip was blunted at the layer interface. The blunted single craze in Figure 1(a) is compared with a craze from a craze doublet in 388 layer PC/SAN (3.6/3.3 μm) and a craze from a craze array in 1857-layer PC/SAN (0.4/1.0 μm) also at a strain of 4.5% in Figure 1(b) and (c). Although the length of the craze, which was determined by the width of the SAN layer, varied from 16 to 3.3 μm to 1.0 μm in these examples, the craze opening where the blunted craze impinged on the PC interface was about 0.5 μm in every case. A similar comparison of crazes at a higher strain, 6.0%, is made in Figure 2. The craze opening increased to about 1.0 μm, but, again, the craze-tip opening was the same in all three examples.

The craze-tip opening measured from scanning electron micrographs of various composites is plotted in Figure 3 as a function of the SAN layer thickness. The crazes gradually widened as the strain increased, as noted previously with a 49-layer composite.[4] Although the thickness of the SAN layers varied by more than an order of magnitude from 0.6 to 16 μm, the craze opening was not affected. The independence of craze-tip opening from craze length was attributed to the presence of load-bearing craze fibrils. At the highest strain included in the plot, 6.0%, the craze opening was in the range reported for bulk crazes.[5]

Hypothesis of Craze Doublet and Craze Array Formation

An important result contained in Figure 3 is that the craze-tip opening is independent of layer thick-

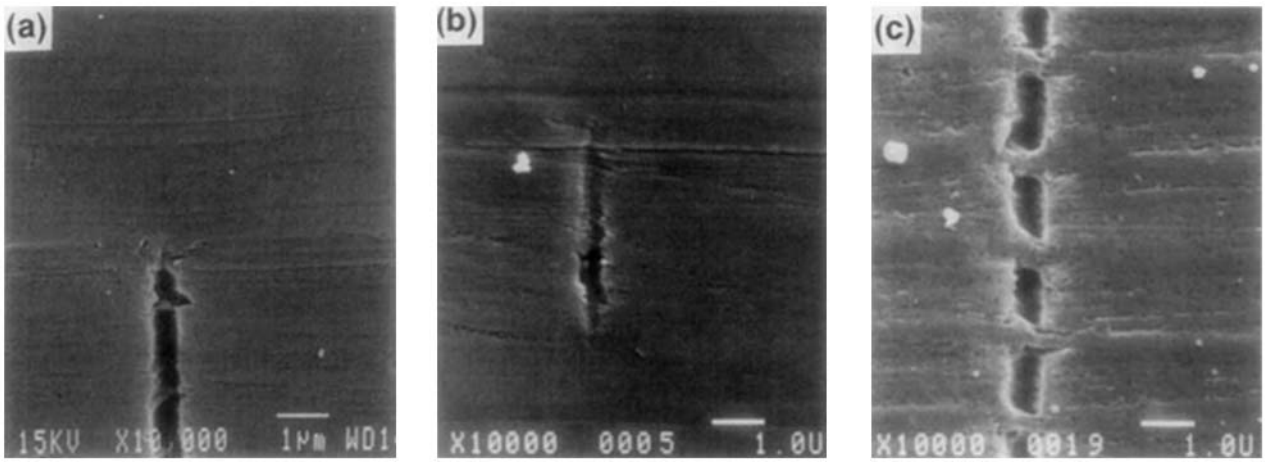

Figure 1 Scanning electron micrographs of crazes at 4.5% strain: (a) a single craze in 49-layer PC/SAN (29/16 μm); (b) a craze from a craze doublet in 388-layer PC/SAN (3.6/3.3 μm); (c) part of a craze array in 1857-layer PC/SAN (0.4/1.0 μm).

ness and depends only on the remote strain. This makes it possible to develop a hypothesis for interactive crazing by considering the size of the craze-tip deformation zone in relation to the thickness of the PC layer. It is assumed that the dimensions of the deformation zone are the same in all composites regardless of layer thickness since these are determined by the magnitude of the craze-tip opening. If the PC layer is relatively thick, the deformation zone will be small compared to the PC layer thickness and its influence will not extend into the PC layer beyond the vicinity of the interface. However, if the thickness of the PC layer is comparable to the dimensions of the deformation zone, the localized stress and strain fields associated with the deformation zone will extend through the PC layer to reach the interface with the next SAN layer. The hypotheses for formation of craze arrays and craze doublets assume that, due to good adhesion, these stress and strain fields are transferred to the next-neighboring SAN layer.

The craze-tip deformation zone in the PC layer consists of a colinear plastic zone together with a pair of micro-shearbands that grow away from the craze tip at an angle of about 45°.[4] A craze array is formed when the PC layer is thin enough for the

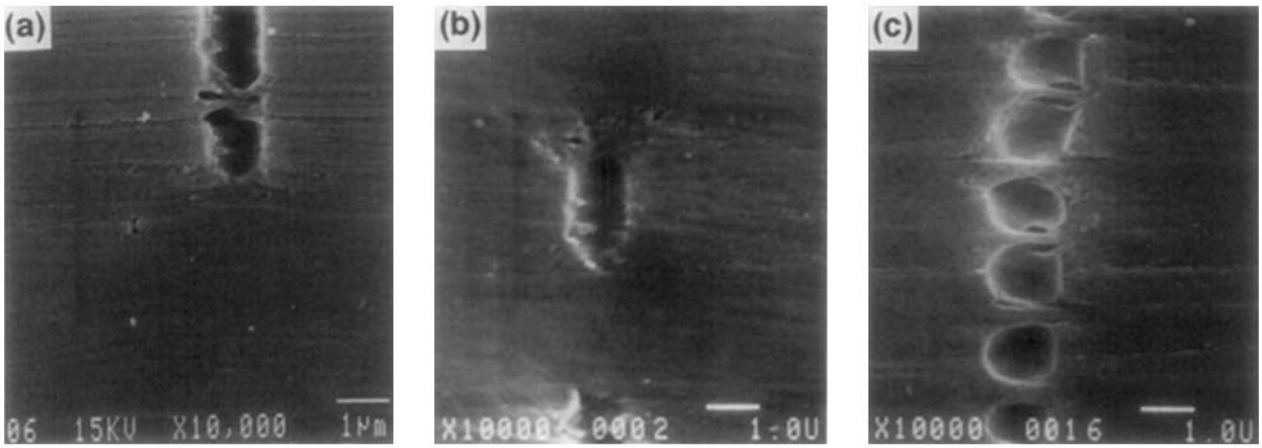

Figure 2 Scanning electron micrographs of crazes at 6.0% strain: (a) a single craze in 49-layer PC/SAN (29/16 μm); (b) a craze from a craze doublet in 388-layer PC/SAN (3.6/3.3 μm); (c) part of a craze array in 1857-layer PC/SAN (0.4/1.0 μm).

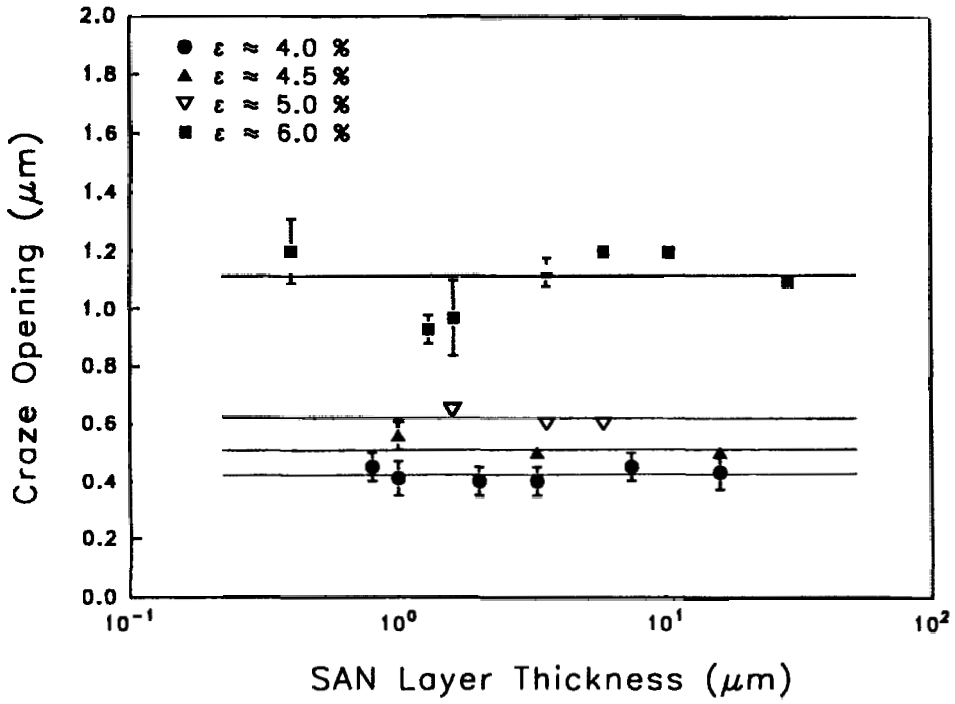

Figure 3 Craze opening measured from scanning electron micrographs at various strains as a function of SAN layer thickness.

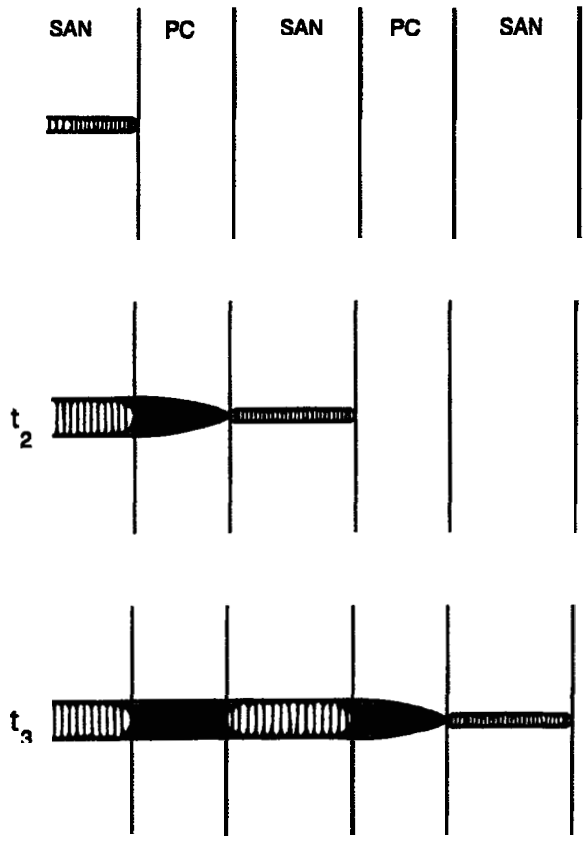

Figure 4 Schematic representation of craze array formation by plastic-zone impingement.

colinear plastic zone to impinge on the interface with the next SAN layer. The schematic in Figure 4 shows how a craze array grows from an initial craze when the colinear plastic zone impinges on the interface with the next SAN layer and initiates a new craze. The process is repeated as the plastic zone from the new craze impinges on the next SAN layer. The crazes are separated by necked ligaments of the PC layers. A craze array could continue to grow indefinitely across the composite normal to the applied stress, and craze arrays with 25 or more crazes are observed. A craze array is terminated when it encounters an unusually thick PC layer, or if it propagates into the vicinity of another craze array that relieves the stress locally, or when the remote stress becomes high enough that micro-shearbanding from the craze tips becomes the dominant deformation mechanism.

The analytical description of the deformation zone developed from a composite with relatively thick PC layers (29 μm) is assumed to be applicable to all PC/SAN microlayer composites. The colinear plastic zone is described by slip-line field theory, and the length of the zone approximately conforms to the theoretical prediction of 2.2 times the craze opening.[4] The zone grows to a maximum length of about 1.3 μm in the thick PC layers before micro-shearbanding begins to dominate. This analysis accurately predicts that composites with PC layers less

Table I Relationship of PC Layer Thickness to Crazing Phenomena

Type of Crazing	Av PC Layer Thickness (μm)	Av SAN Layer Thickness (μm)	Percentage of Crazes in Doublets or Arrays (%)	No. Layers
Single crazes	29	16	0	49
	27	17	0	49
	23	27	0	49
	13	33	0	49
	10	3.3	0	194
	7.5	5.2	0	194
Craze doublets	5.9	7.5	16	194
	4.4	9.3	16	194
	3.6	3.3	13	388
	1.9	1.0	18	776
	1.6	0.8	14	927
	1.5	1.2	13	776
Transitional	1.3	2.0	60	776
Craze arrays	0.8	1.6	95	927
	0.7	0.6	96	1857
	0.4	1.0	97	1857

than 1.3 μm thick exhibit craze arrays (Table I). Crazing of a microlayer composite with PC layers 1.3 μm thick is transitional with about 60% of the crazes in short craze arrays; the percentage of crazes in arrays increases to close to 100% when the PC layer thickness is less than 1 μm.

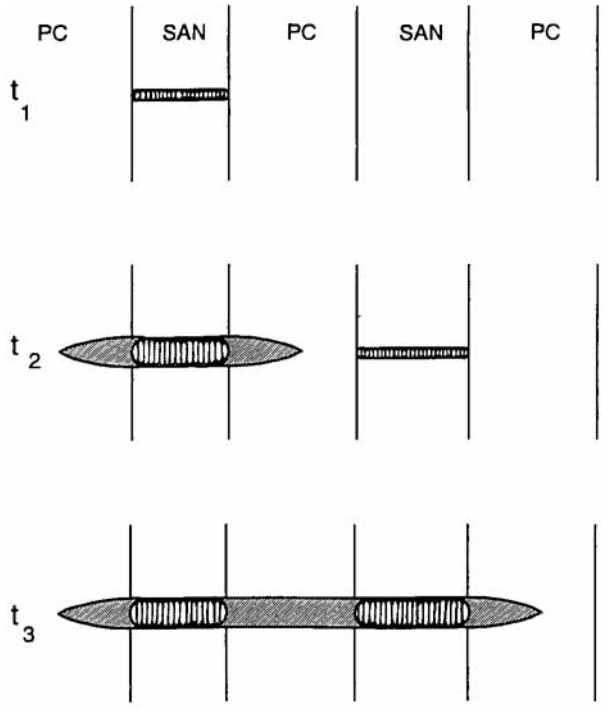

Figure 5 Schematic representation of craze doublet formation by elastic stress intensification.

It is not necessary for the PC layer to be so thin that the plastic deformation actually impinges on the interface for the deformation zone to affect the next SAN layer. The intensified elastic stress field ahead of the plastic zone is felt at the interface before the plastic deformation reaches the interface. The result of the intensified elastic stress is an increased probability that a second craze will initiate in the neighboring SAN layer. A craze doublet is created when the second craze initiates at the position where the stress intensification is highest, as shown schematically in Figure 5. Not all crazes produce craze doublets; only about 20–30% of the crazes are in craze doublets in those composites with PC layer thickness between 1.3 and 6.0 μm where craze doublets are observed.[1] The probability of a second craze forming as a result of the stress intensification is related to the Weibull relationship between craze density and stress in the SAN layer.

Distribution of Craze Doublets

The correlation length was again used to characterize the location of crazes relative to one another. As described previously,[4] the correlation length (R) was defined as the perpendicular distance between two

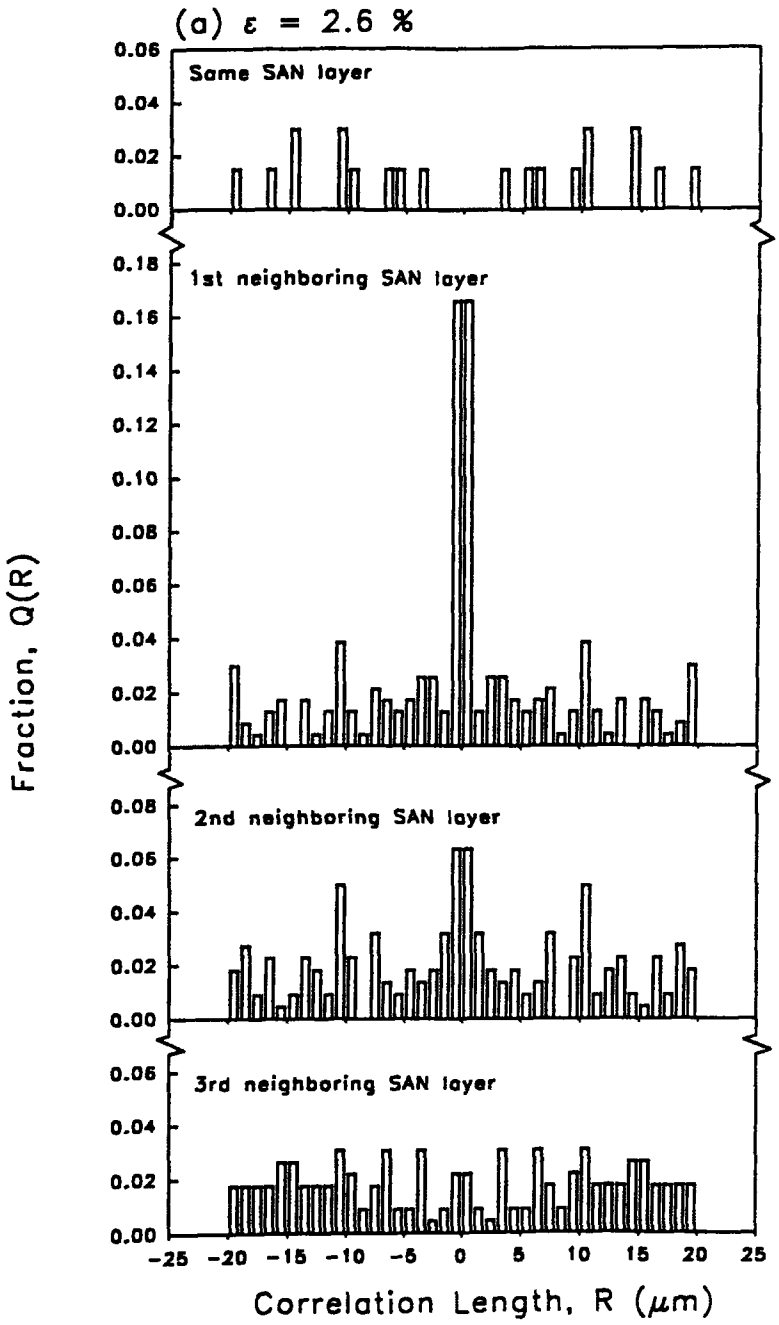

Figure 6 Distribution of craze correlation lengths in the same SAN layer, and the first-, second-, and third-neighboring SAN layers in 194-layer PC/SAN (4.4/9.3 μm): (a) 2.6% strain with 239 crazes counted; (b) 2.9% strain with 522 crazes counted.

crazes; the length unit of R was 1 μm. The craze positions relative to a reference line were measured from photomicrographs and the correlation lengths were determined for $R \leq 60$. The absolute values were sorted into correlation lengths between crazes in the same SAN layer, the first-neighboring SAN layers, the second-neighboring SAN layers, etc. In each of the sorted categories, the probability of a particular R value was then given by

$$Q(R) = N(R)/N_t \quad (1)$$

where $N(R)$ is the total number of correlation

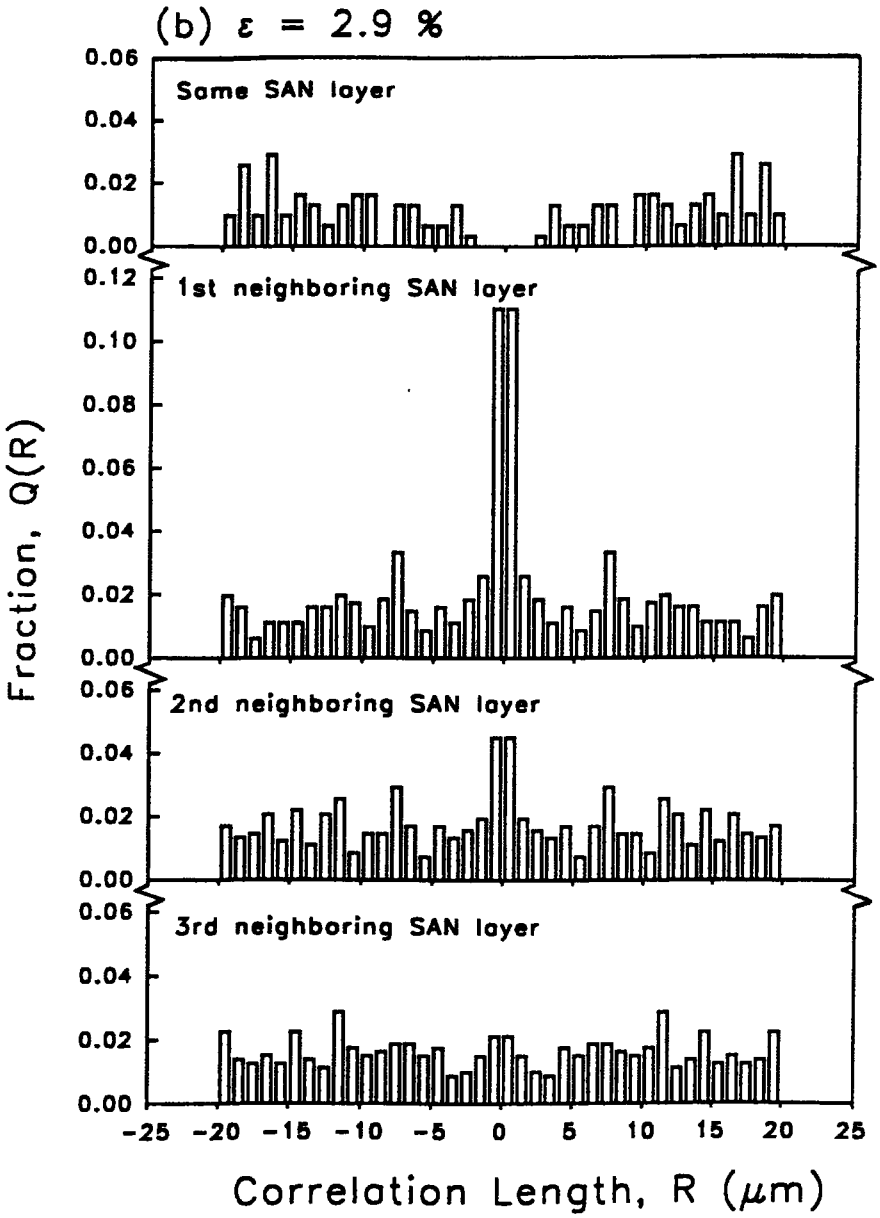

Figure 6 *(Continued from the previous page.)*

lengths having a value R, and N_t, the sum of all the $N(R)$'s for correlation lengths between 0 and 60.

The probabilities of R values between 0 and 20 for two composites with PC layer thicknesses in the 1.3–6.0 μm range, 194-layer PC/SAN (4.4/9.3 μm) and 388-layer PC/SAN (3.6/3.3 μm), are plotted in Figures 6 and 7. Since negative and positive R values were indistinguishable, the region close to $R = 0$ was emphasized by plotting $Q(R)$ vs. both $+R$ and $-R$. The figures include probabilities for correlation lengths between crazes in the same SAN layer and the first-, second-, and third-neighboring SAN layers. If crazing occurred randomly, the probability would be 1/60 or 0.0167. A higher value would indicate stress intensification, and a lower value, stress reduction. The low probability of finding two crazes close together in the same layer was also observed in the composite with thicker layers, 49-layer PC/SAN (29/16 μm), and was attributed to localized stress relief.[6] Alignment of crazes in neighboring SAN layers was indicated by a $Q(R)$ value higher than 0.0167 at $R = 0$ in the distribution of correlation lengths for the first-neighboring SAN layer. The presence of craze doublets is shown in Figures 6 and

7 by the high probability of a correlation length $R = 0$ between crazes in the first-neighboring SAN layer. Furthermore, the higher than random probability for $R = 0$ between crazes in the second-neighboring SAN layer indicated that some craze triplets were formed. In general, no arrays larger than triplets formed since $Q(R)$ for $R = 0$ was usually the same as the random probability for crazes in the third-neighboring SAN layer.

The probability of craze doublets changed with strain and also depended on the thickness of the PC layer. These effects were described by a probability factor $I(R)$ defined as

$$I(R) = Q(R = 0)/0.0167 \qquad (2)$$

which compared the probability of aligned crazes to the random probability. The probability factor for craze doublets in the PC/SAN (4.4/9.3 μm) composite (Fig. 6) was 10 at a strain of 2.6% and decreased to 4 at 2.9% strain; for craze triplets, the probability factor decreased from 4 to 3. Similarly, for the PC/SAN (3.6/3.3 μm) (Fig. 7), the corresponding decreases were from 16 to 7 for craze doublets and 10 to 3 for triplets. This meant that the probability of a craze being part of a doublet was higher at a low strain when the number of crazes was small. When the strain increased, it became more likely that new crazes would form as single crazes rather than as part of craze doublets. The probability factor was also higher for the composite with the thinner PC layers because the tip of the plastic zone was closer to the interface.

Simulation of Craze Doublets

The merit of the stress-intensification hypothesis for craze doublet formation was tested by carrying out a calculation derived from the statistical nature of crazing in noninteracting SAN layers of the 49-layer composite.[4] Starting with the random distribution of crazes in the 49-layer composite, additional crazes were assigned to some of the positions of stress intensification, i.e., positions in the next-neighboring SAN layer aligned with existing crazes. Several values for the stress intensification were chosen and the number of crazes to be added was determined from the Weibull distribution. The one-dimensional coordinates of the added crazes were combined with the others, and the correlation lengths were calculated as described previously. The calculated correlation length distributions were compared with those obtained from experiments on composites that exhibited craze doublets.

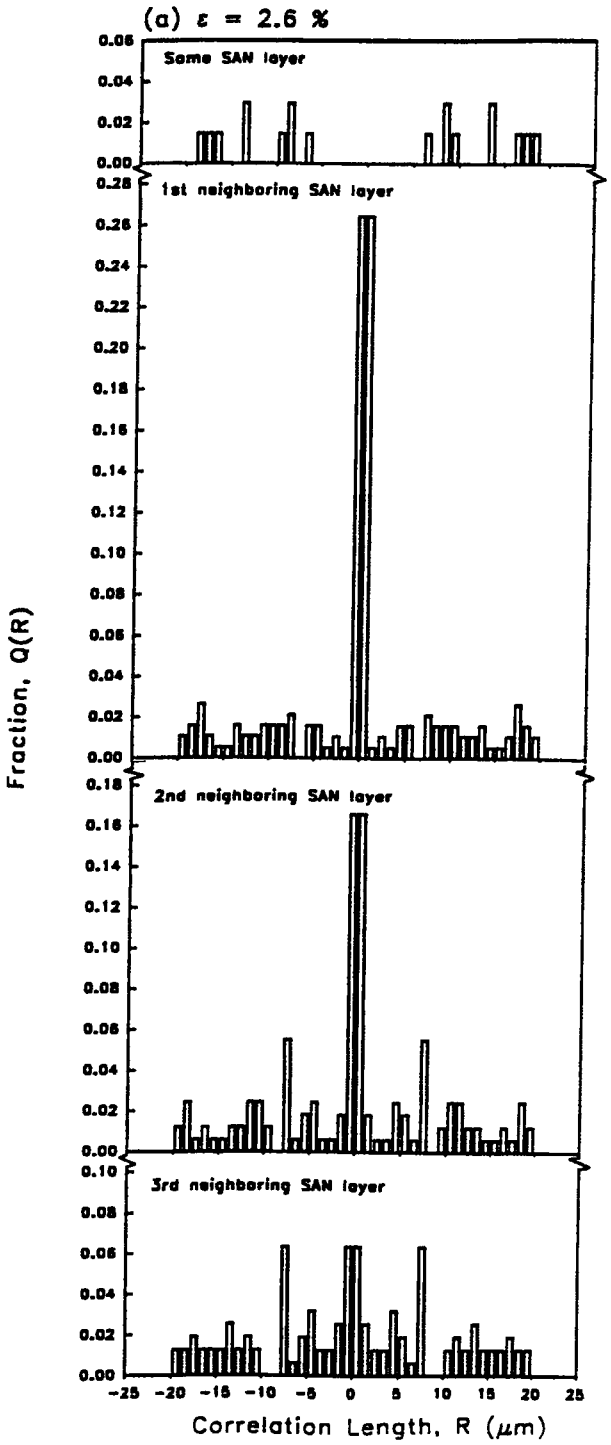

Figure 7 Distribution of craze correlation lengths in the same SAN layer, and the first-, second-, and third-neighboring SAN layers in 388-layer PC/SAN (3.6/3.3 μm): (a) 2.6% strain with 190 crazes counted; (b) 3.0% strain with 232 crazes counted.

Data from the 49-layer composite at two strains, 2.7 and 3.0%, were chosen for this exercise. Since the coordinates of the crazes were measured to the

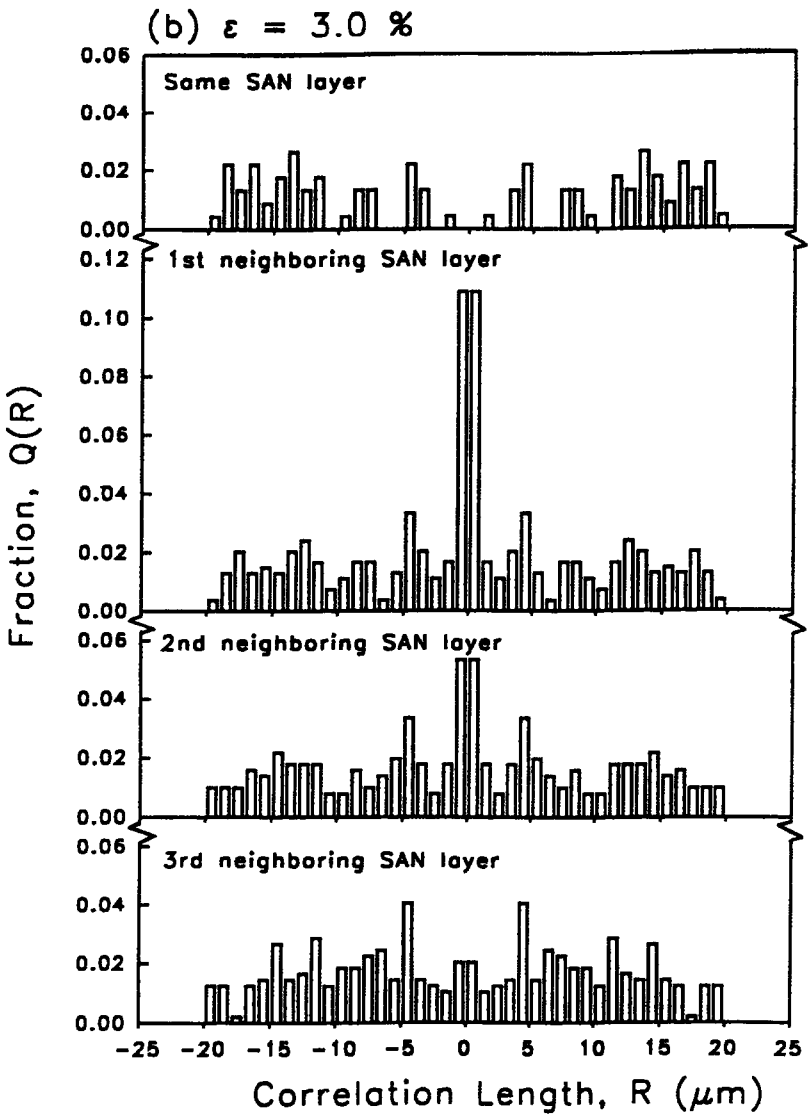

Figure 7 *(Continued from the previous page.)*

Table II Parameters for Simulation of Craze Doublets

Remote Strain	K	σ_{SAN}[a]	F_C[a]	N_K	N_C	$2N_K/N_C$
2.7[b]	1.00	49.0	0.08	0	431	0
	1.03	50.5	0.10	62	493	0.25
	1.05	51.5	0.13	80	511	0.31
	1.08	52.9	0.20	123	554	0.44
3.0[c]	1.00	54.0	0.23	0	474	0
	1.03	55.6	0.26	88	562	0.31
	1.05	56.7	0.28	93	567	0.33
	1.08	58.3	0.31	105	579	0.36

E_T: total no. elements; N_0: no. crazed elements; E_K: no. stress-intensified elements; K: stress-intensification factor; F_C: craze fraction; N_K: no. crazes in stress-intensified elements; N_C: total no. crazed elements; $2N_K/N_C$: fraction of crazes in craze doublets.

[a] Taken from the Weibull plot in Ref. 4.

[b] $E_T = 7140$, $N_0 = 431$, $E_K = 817$.

[c] $E_T = 6630$, $N_0 = 474$, $E_K = 948$.

nearest micron, the SAN layers were divided into elements 1 micron in length, each of which potentially could contain a craze. The total number of elements (E_T) and the number of crazed elements (N_0) were determined, and the number of elements experiencing a stress intensification (E_K), i.e., two for each existing craze except for crazes in the edge layers where there was only one, was calculated. The simulation required the element size to be small enough that most of the elements would not contain crazes. The 1 micron element size met this condition with only 6–7% of the elements occupied by crazes.

The number of stress-intensified elements that contained crazes for a given stress intensification factor K was determined with reference to the Weibull plot.[4] This plot provided the relationship between the stress in the SAN layer and the craze fraction (F_C) defined as the number of crazes formed at a given stress relative to the total number of crazes in the fully crazed composite. Values of F_C for several levels of stress intensification are given in Table II. If the stress was increased from σ_{SAN} to $K\sigma_{SAN}$, the craze fraction would increase from F_{C0} to F_{CK} and the number of the E_T elements that contained crazes

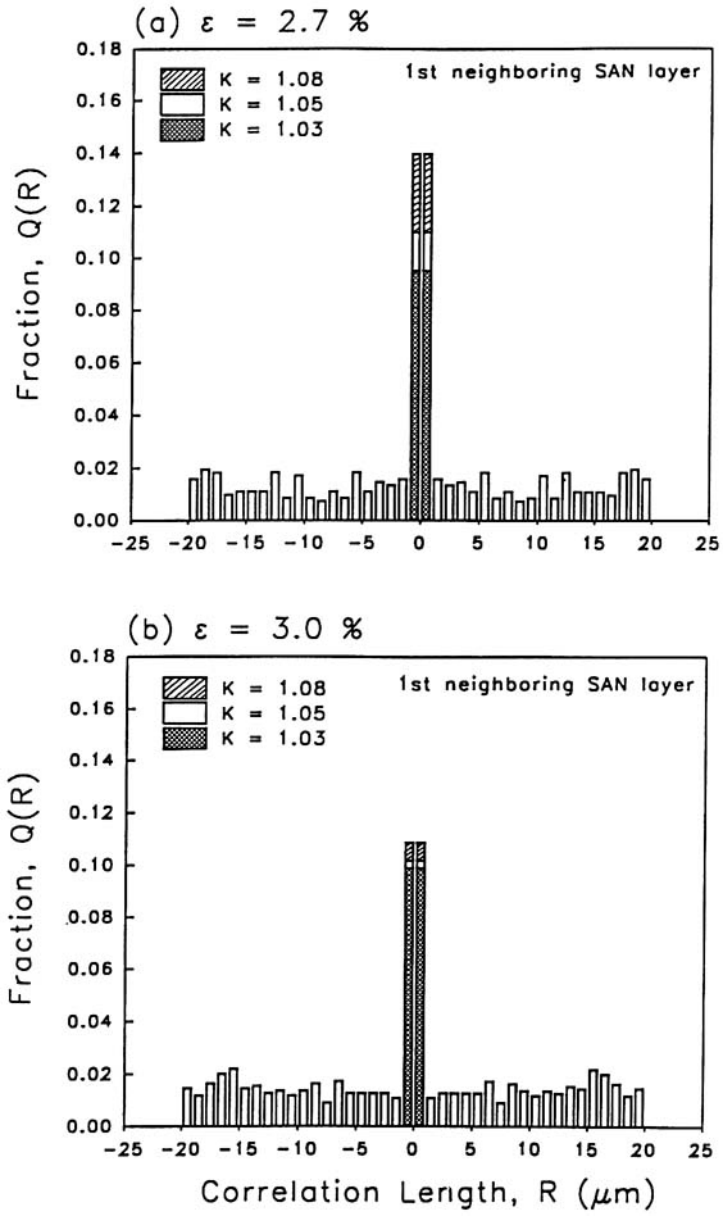

Figure 8 Calculated distribution of craze correlation-lengths in the first-neighboring SAN layer: (a) 2.7% strain; (b) 3.0% strain.

would increase from N_0 to $N_0(F_{CK}/F_{C0})$. In the simulation, only E_K elements experienced stress intensification; of these E_K elements, the number that contained crazes was then given by

$$N_K = (E_K/E_T)N_0(F_{CK}/F_{C0}) \quad (3)$$

Values obtained for the number of stress intensified elements crazed (N_K), the total number of crazed

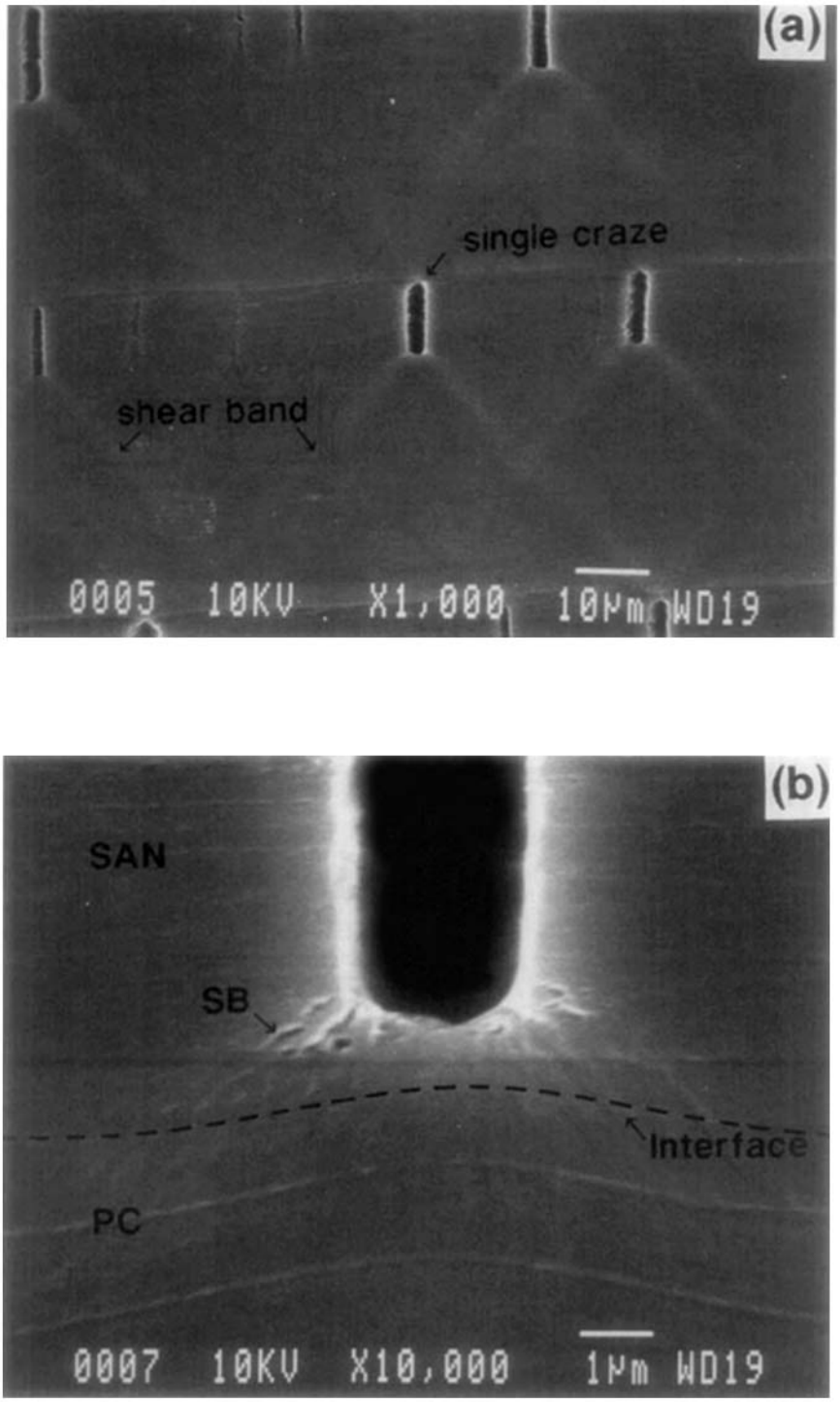

Figure 9 Scanning electron micrographs of 49-layer PC/SAN (29/16 μm): (a) low magnification of the micro-shearbands; (b) higher magnification of the PC/SAN interface.

elements (N_C), and the resulting fraction of crazes in craze doublets ($2N_K/N_C$) are included in Table II.

For the sample calculation at the lower strain (2.7%), the effect of increasing the stress intensification factor from 1.03 to 1.08 had the effect of increasing the fraction of crazes in craze doublets from 0.25 to 0.44. The magnitude of the stress intensification did not have as large an effect at the higher strain (3.0%) where the same increase in

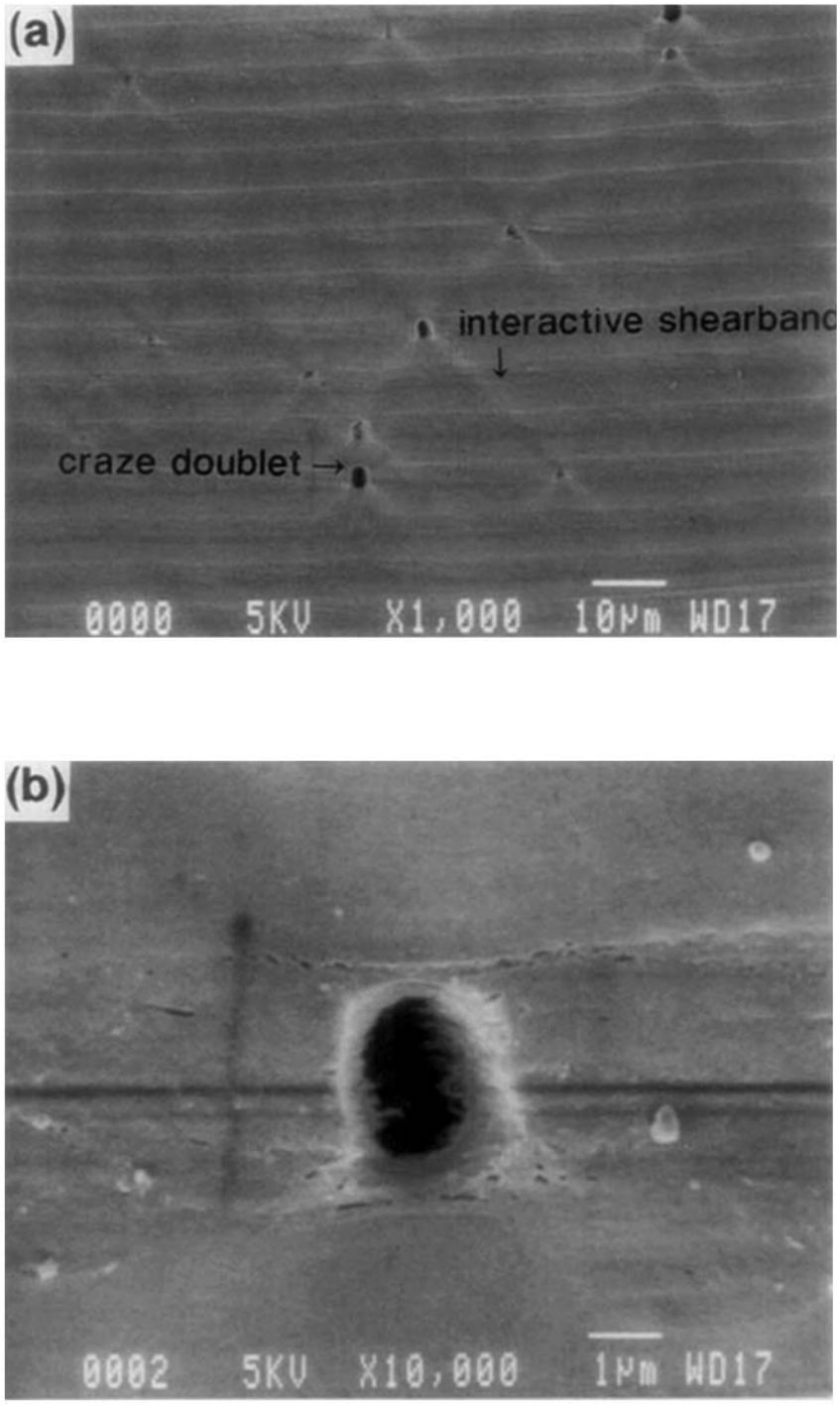

Figure 10 Scanning electron micrographs of 388-layer PC/SAN (3.6/3.3 μm): (a) low magnification of the micro-shearbands; (b) higher magnification of the PC/SAN interface.

stress intensification factor caused the fraction of crazes in craze doublets to increase from 0.31 to 0.36. A stress-intensification factor in the range of 1.03–1.05 predicted a craze doublet fraction comparable to that observed experimentally; for example, the observed fractions were 0.29 (2.6% strain) and 0.27 (2.9% strain) for the PC/SAN (4.4/9.3 μm) composite and 0.30 (2.6% strain) and 0.34 (3.0% strain) for the PC/SAN (3.6/3.3 μm) composite.

The N_K additional crazes were randomly assigned positions in the E_K stress-intensified elements, the one-dimensional coordinates of the added crazes were combined with those of the N_0 random crazes, and the correlation lengths were calculated as described previously. The calculated correlation length distributions for the first-neighboring SAN layer at two strains are plotted in Figure 8. They closely resemble the experimental distributions, as was expected since the fraction of crazes in craze doublets in the simulation was about the same as observed experimentally.

Micro-Shearbands and Yielding

When the strain exceeded about 4.5%, there was a distinct lessening in the formation of new crazes, while growth of micro-shearbands from existing craze tips became much more noticeable. A close examination of the interface region at the craze tip revealed that a typical craze terminated a short distance inside the SAN layer (Figs. 9 and 10). It appeared that the micro-shearbands initiated from the blunted craze tip a short distance inside the SAN layer and grew through the interface into the PC layer. Considerable distortion sustained by the interface as a result of the micro-shearbanding attested to the good adhesion between PC and SAN.

It was determined in the 49-layer composite, where the micro-shearbands did not penetrate to the interface with the next SAN layer, that the length of the micro-shearbands depended on the craze-tip opening and the applied stress.[4] Since the craze-tip opening was observed to be independent of layer thickness, it follows that the length of the micro-shearbands also should not depend on layer thickness. Micrographs of 49-layer PC/SAN (29/16 μm) and 388-layer PC/SAN (3.6/3.3 μm) at similar strains close to the yield point are compared in Figures 9 and 10. Although lengths were difficult to measure in the 388-layer composite because the micro-shearbands extended across layer interfaces and interacted with micro-shearbands from other crazes, it was apparent that the length, about 20 μm, and the angle, about 45°, were comparable to those in the 49-layer composite.

Models that describe the micro-shearband length were previously tested with data from the composite with thick PC layers.[4] The micro-shearband length (L_h) at several stresses close to the yield point as predicted by the BCS model,[7]

$$L_h/a = \sec(\pi\sigma/2\sigma_y) - 1 \qquad (4)$$

and by the Vitek model,[8]

$$L_h/a = 0.015 \exp[6.642(\sigma/\sigma_y)] \qquad (5)$$

are compared with the PC layer thickness of 49-layer PC/SAN (29/16 μm) and 388-layer PC/SAN (3.6/3.3 μm) in Figure 11. Both models predict that the micro-shearbands do not reach the next interface in the 49-layer composite, whereas in the 388-layer composite, the micro-shearbands grow through the PC layer and into the next SAN layer before the composite yields. The BCS model, which appears to give the best representation of micro-shearband length at higher stresses,[4] suggests that when the stress reaches 98% of the yield stress the micro-shearbands have grown through three or four layers.

Growth of micro-shearbands was followed by instability and global necking. When the 49-layer PC/SAN (29/16 μm) composite reached the yield in-

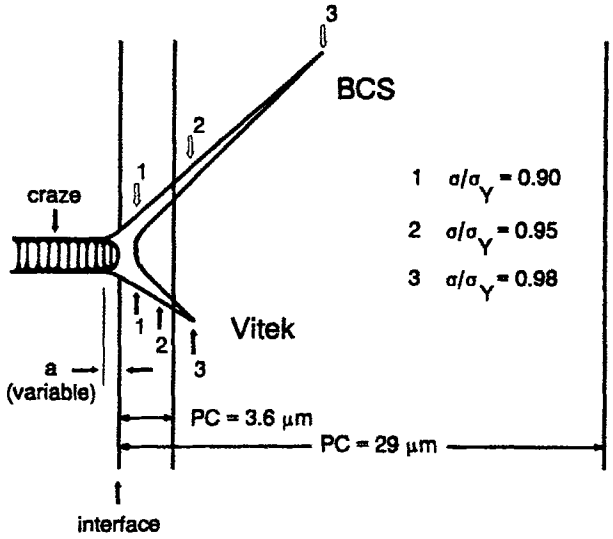

Figure 11 Calculated micro-shearband length from eqs. (4) and (5) at three remote stress levels compared with the PC layer thickness of 49-layer PC/SAN (29/16 μm) and 388-layer PC/SAN (3.6/3.3 μm).

stability at about 6% strain, the SAN crazes opened up to accommodate localized extension of the PC layers. During craze opening, the craze fibrils fractured with the result that the load-bearing craze was replaced by a void (Fig. 12). During necking, the width of the PC layers decreased by about 25%, but there was little change in the width of the SAN layers since deformation of the SAN layers consisted primarily of opening of the voids. As the craze opened, the craze tip penetrated into the PC layer and the shape of the craze changed from cracklike to hexagonal. Opening of the voids led to tearing fracture of the PC layers. As a consequence of the tearing fracture from voids in the SAN, conventional tensile specimens of this composite did not exhibit stable neck propagation but fractured after the necking instability was achieved.

The micro-shearbands in 388-layer PC/SAN (3.6/3.3 μm) grew through the PC layers and extended into several adjacent SAN and PC layers. During neck formation, the crazes did not open up into voids (Fig. 13); instead, the SAN layers extended uniformly between the crazes and thinning of both PC and SAN layers was observed. This change in the deformation mechanism in the SAN layers at the yield instability, from craze opening to shear yielding, was a consequence of impingement of the micro-shearbands on the PC/SAN interface and subsequent propagation of the micro-shearband into and through the SAN layer. The change in deformation mechanism of the SAN at the yield point resulted in formation and propagation of a stable neck. Conventional tensile specimens of microlayer composites with thin layers were distinctly more

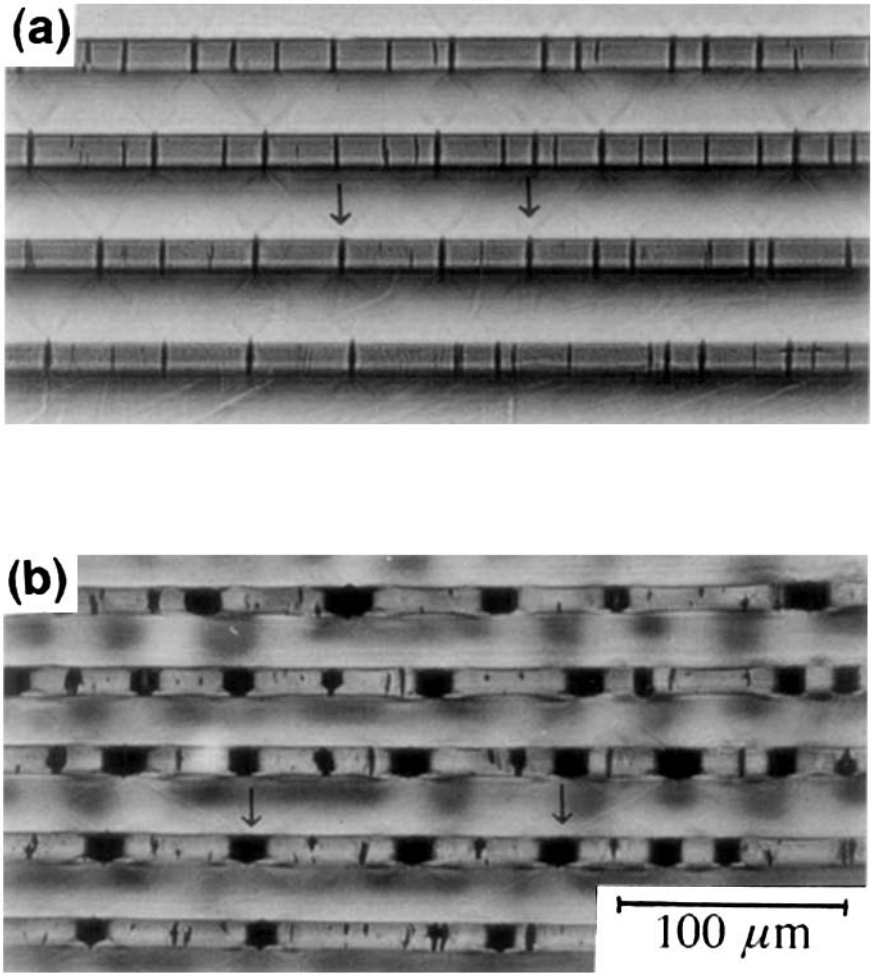

Figure 12 Optical micrographs of 49-layer PC/SAN (29/16 μm): (a) before necking; (b) the same region after necking. The arrows identify the same two crazes in both micrographs.

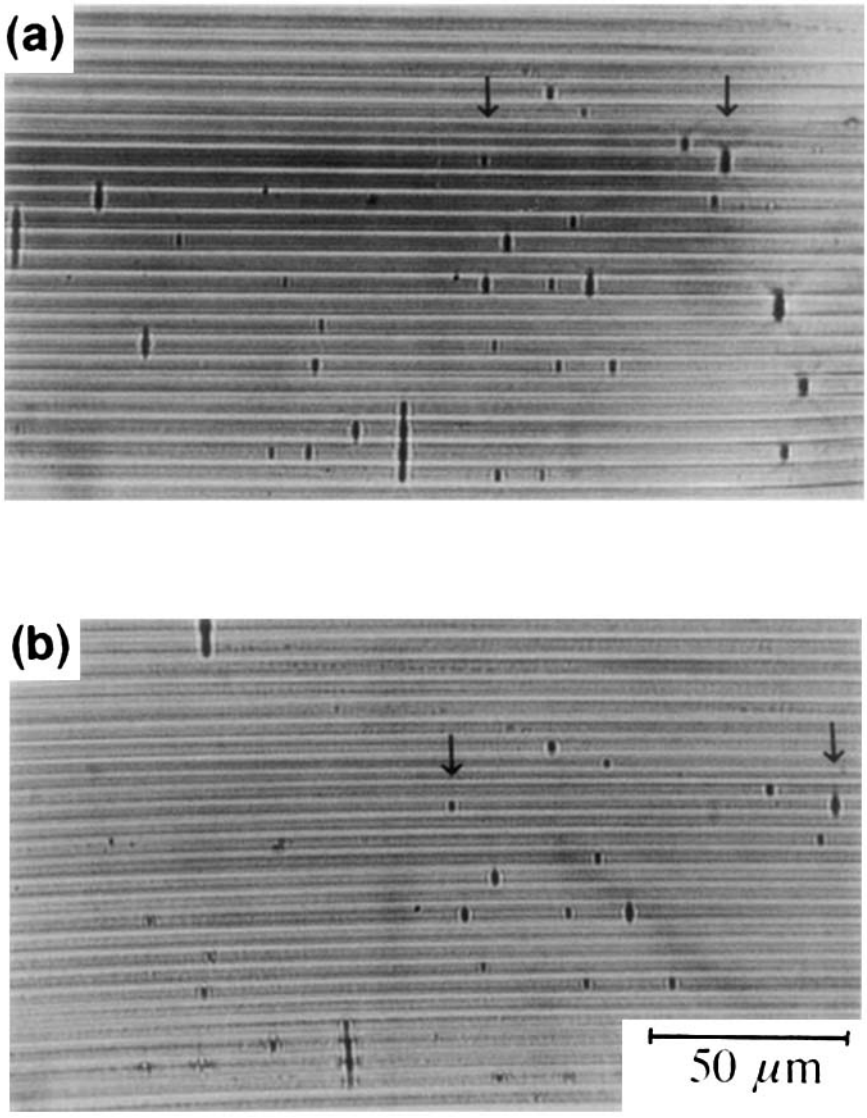

Figure 13 Optical micrographs of 388-layer PC/SAN (3.6/3.3 μm): (a) before necking; (b) the same region after necking. The arrows identify the same two crazes in both micrographs.

ductile than were composites of the same PC/SAN composition but with thicker layers.

CONCLUSIONS

The concept of the craze-tip deformation zone is used to explain interactive crazing and micro-shear-banding in PC/SAN microlayer composites. The zone that forms in the PC layer consists of a colinear plastic zone together with a pair of micro-shearbands that grow at an angle of about 45°. It is shown that when the PC layer is thin enough the deformation zone can interact with the next-neighboring SAN layer. This led to the following conclusions:

1. Since the craze-tip opening does not depend on the SAN layer thickness, the size and shape of the resulting deformation zone also do not depend on the layer thickness.
2. When the PC layer is less than 6 μm thick, the elastic stress concentration from the co-linear plastic zone increases the probability of crazing in the neighboring SAN layer with

the formation of craze doublets that consist of two aligned crazes in neighboring SAN layers.

3. When the PC layer thickness is less than 1.3 μm, the length of the colinear plastic zone is comparable to the PC layer thickness; formation of a craze at the point of impingement on the neighboring SAN layer leads to craze arrays with many aligned crazes in neighboring layers.
4. When the layers are thin enough, the microshearbands grow through the PC layers and extend into several adjacent SAN and PC layers; this produces a change in deformation mechanism in the SAN layers at the yield instability from craze opening to shear yielding.

The authors wish to thank Dr. S. Bazhenov of the Institute of Chemical Physics, USSR Academy of Science, Moscow, USSR, and Dr. J. Im of The Dow Chemical Co., Midland, MI, for numerous technical contributions. This research was generously supported by the National Science Foundation, Polymers Program (DMR 9100300).

REFERENCES

1. D. Haderski, K. Sung, J. Im, A. Hiltner, and E. Baer, *J. Appl. Polym. Sci.*, **52,** 121 (1994).
2. M. Ma, K. Vijayan, J. Im, A. Hiltner, and E. Baer, *J. Mater. Sci.*, **25,** 2039 (1990).
3. A. Hiltner, K. Sung, E. Shin, S. Bazhenov, J. Im, and E. Baer, *Mater. Res. Soc. Symp.*, **255,** 141 (1992).
4. K. Sung, D. Haderski, A. Hiltner, and E. Baer, *J. Appl. Polym. Sci.*, **52,** 135 (1994).
5. G. H. Michler, *J. Mater. Sci.*, **25,** 2321 (1990).
6. J. Im, A. Hiltner, and E. Baer, in *High Performance Polymers,* E. Baer and A. Moet, Eds., Hanser, New York, 1991, p. 175.
7. B. A. Bilby, A. H. Cottrell, and K. H. Swinden, *Proc. R. Soc. A,* **272,** 304 (1963).
8. V. Vitek, *J. Mech. Phys. Solids,* **24,** 263 (1976).

Received June 21, 1993
Accepted August 9, 1993